Engineering 6 (2020) 1019–1027

Contents lists available at ScienceDirect

Engineering

journal homepage: www.elsevier.com/locate/eng

Research
Energetic Materials and Interdisciplinary Science—Article

Enhancing the Combustion Performance of Metastable Al@AP/PVDF Nanocomposites by Doping with Graphene Oxide

Shuwen Chen, De-Yun Tang, Xue-Xue Zhang, Jie-Yao Lyu, Wei He, Peijin Liu, Qi-Long Yan *

Science and Technology on Combustion, Internal Flow and Thermostructure Laboratory, Northwestern Polytechnical University, Xi'an 710072, China

ARTICLE INFO

Article history:
Received 27 September 2019
Revised 17 January 2020
Accepted 25 February 2020
Available online 12 August 2020

Keywords:
Metastable intermixed composites
Al@AP/PVDF nanocomposites
Graphene oxide
Energy output
Combustion characteristics

ABSTRACT

A new group of energetic metastable intermixed composites (MICs) was designed and fabricated by means of the spray granulation technique. These MICs are composed of aluminum (Al) as the fuel, ammonium perchlorate (AP) and polyvinylidene fluoride (PVDF) as the co-oxidizer. The AP/PVDF ratio was optimized by taking the maximum energy release as the criteria. A minor content of graphene oxide (GO) was also doped in the MICs to act as both lubricant and catalyst. It was shown that Al@AP/PVDF with 0.2% GO has the greatest density (2.57 $g \cdot cm^{-3}$) and highest heat of reaction (5999.5 $J \cdot g^{-1}$). These values are much higher than those of Al@AP/PVDF (2.00 $g \cdot cm^{-3}$ and 5569.8 $J \cdot g^{-1}$). The inclusion of GO increases the solid-state reaction rate of Al@AP/PVDF and improves the thermal stability. The flame propagation rate was increased up to 4.76 $m \cdot s^{-1}$ by doping with 0.2% GO, and was about 10.7% higher than that of Al@AP/PVDF. Al@AP/PVDF-GO has a better interfacial contact and particle distribution, which results in an improved heat-transfer rate, freedom from the agglomeration of nano-Al particles, and an improved combustion reaction rate. This work demonstrates a new strategy to improve the energy release rate and combustion efficiency of Al-based MICs.

1. Introduction

Metastable intermixed composites (MICs) are a typical group of energetic materials (EMs), composed of oxidizers and fuels at the nanoscale [1,2]. MICs are known for their advantages of high energy density and fast energy release rate, and are widely used for propulsion and energy-storage devices [3–5]. Many types of structures can be applied to form new MICs, through the introduction of special fabrication approaches. In the past few decades, novel "layer-by-layer" or "core–shell" structures [6], three-dimensional (3D) ordered macroporous-structured [7], and ternary nanocomposites [8] have been prepared and investigated, and have been found to be effective for tailoring the ignition and combustion properties. It has also been found that the use of advanced preparation methods may optimize the safety and cost of the corresponding MICs [1]. For example, the combustion performance, ignition characteristics, and safety can be controlled well using different strategies. Aluminum (Al) powder is widely used as the fuel in EMs due to its high energy content and low toxicity [9]. Decreasing the particle size of Al to the nanoscale increases the burning rate greatly and significantly decreases the ignition delay [10,11]. However, nano-Al (n-Al) has a significant drawback: It easily forms a significant amount of aluminium oxide (Al_2O_3) shell during long-term storage, which results in a loss of energy content and reactivity. Furthermore, because of its high specific surface area, it is easy for the nanoscale particles to be agglomerated, resulting in a decrease in reaction rate and energy release efficiency. This issue has attracted attention from many researchers, who have focused on modifying the surface of n-Al to enhance its reactivity during ignition, while providing a passivation effect during storage. In our previous work [12–14], various new types of core–shell-structured Al-based MICs with tunable reactivity through the use of different interfacial layers were prepared by *in situ* synthetic methods, and showed an excellent energy release rate and reduced sensitivity. For applications in composite propellants, ammonium perchlorate (AP) is usually used as the oxidizer filler due to its high oxygen content and low cost [15]. The addition of AP can improve the Al combustion performance.

In nitrate ester plasticized polyether (NEPE) propellants, Fang and Li [16] added superfine aluminum powder into the NEPE system, resulting in better combustion characteristics and higher

* Corresponding author.
E-mail address: qilongyan@nwpu.edu.cn (Q.-L. Yan).

https://doi.org/10.1016/j.eng.2020.02.014
2095-8099/

combustion efficiency due to the interaction of AP with Al. Li et al. [17] considered the effect of AP and Al in hexanitrohexaazaisowurtzitane (CL-20)/NEPE propellant systems, and found that AP increased the oxygen coefficient and burning rate, while Al powder also increased the burning rate. In a system of n-Al/AP-based composite propellants using hydroxyl-terminated polybutadiene (HTPB) as a binder, the reactions between the n-Al and AP improved the specific impulse [18] and increased the burning rates [19]. AP/Al/HTPB propellants have excellent thermal stability, low impact sensitivity, and good mechanical properties [20,21].

Nitrocellulose (NC) is also often used as an energetic binder in n-Al/AP systems, resulting in a lower ignition temperature and a higher flame temperature [22]. The thermal mechanism of Al/AP/NC was clarified by Wang et al. [22], who showed that the alumina shell first reacts with the AP, and then the reaction between the Al and NC takes place. Al/AP was also used to fabricate NC/nitroglycerin (NG)/AP/Al as a composite modified double-base propellant; the mechanical properties were clearly improved, due to the cross-linking structure of the binder [23]. Furthermore, fluorine-based polymers were chosen as the reactive binders to replace NC or HTPB in order to improve the combustion efficiency of Al while decreasing agglomeration. The combination of Al with fluorine-based polymers (e.g., polyvinylidene fluoride (PVDF) and polytetra fluoroethylene (PTFE)) also increased the reaction rate and the combustion efficiency, the latter due to decreased condensed products [24,25].

Moreover, in order to further enhance the combustion performance of MICs, researchers considered using carbon nanotubes (CNTs) [26] and graphene oxide (GO) [27] as combustion catalysts and lubricants in the composition of MICs. In particular, it was shown that Al/PTFE doped with CNTs has a better energy output, faster combustion speed, and tunable ignition delay time depending on the content of CNTs [26]. The electrospinning technique was introduced to fabricate PVDF/CuO/Al composite membranes doped with GO, which showed a higher density, higher reaction heat, and improved combustion performance [27].

In order to further improve the combustion performance of conventional Al/PVDF MIC, and make it more suitable as a promising ingredient for solid propellants, both AP and GO were used in the present work to fabricate various new types of MICs with better performance. Due to the severe agglomeration that occurred among nanoscale Al particles during the fabrication of these composites, the spray granulation technique was used in order to obtain composites with better homogeneity and dispersion. This was expected to improve the long-term storage stability, safety, and combustion efficiency of these MICs. The effect of the GO mass content (0, 0.1%, 0.2%, or 0.5%) on the thermal behavior and combustion performance of Al@AP/PVDF was evaluated, and the thermal decomposition and flame propagation speeds were characterized in detail.

2. Experiments

2.1. Materials

All the materials were purchased and used as received. AP (purity > 99.5%) was obtained from Xi'an Modern Chemistry Research Institute. N-Al powder (80 nm, purity > 99.9%) was supplied by Novacentrix Company. The active aluminum content was about 80%, as measured by thermal gravimetric analysis (TGA). PVDF (Kynar 761, purity > 99.9%) was purchased from Arkama Incorporation. The commercial GO (1–3 layers, oxygen content > 42%) was produced by Nanjing JCNANO Technology Co., Ltd. *N*,*N*-dimethylformamide (DMF, 99.5%) was obtained from Beijing Chemical Reagent Company.

2.2. Sample preparations

The PVDF powder was dissolved in DMF and stirred magnetically for 12 h at 40 °C. Next, AP and n-Al powder were dispersed in the pre-prepared PVDF solution, followed by 1 h of ultrasonic dispersion and 24 h of magnetic stirring at room temperature. The final homogeneous suspension was then used for spray granulation.

For GO-modified Al@AP/PVDF composites, GO was first dispersed in DMF by ultrasonic dispersion for 1 h. Next, the GO suspension was added dropwise into the PVDF solution. After 1 h of stirring, AP and n-Al powder were dispersed into the PVDF-GO solution. The resulting uniformly mixed solution was then used for spray granulation.

The suspension of the abovementioned mixture at the designed stoichiometry was used to prepare core–shell structured particles at a spray-drying facility (YC-015, Yacheng Yiqi, China). And the composite particles were collected in a connected glass vessel without further treatment.

2.3. Characterization techniques

Evo 18 (Sigma, ZEISS, Germany) was used to characterize the morphology of the Al@AP/PVDF-GO composites with 10 mm working distance at 15 kV accelerating voltage. The heat of reaction was measured by means of standard oxygen bomb calorimetry (ZDHW-HN7000C, Huaneng Keji Co., Ltd., China) with an argon pressure of 3.0 MPa. The reaction residues from the bomb calorimetry were characterized using an X-ray diffractometer (XRD, Xpert Pro MPD, Panalytical, the Netherlands) to determine the component after the combustion process. The thermal properties of Al@AP/PVDF-GO were studied using a simultaneous TGA/differential scanning calorimeter (DSC) instrument (STA449 F5, NETZSCH, Germany) with 40 $mL \cdot min^{-1}$ of argon flow from 40 to 1000 °C at a heating rate of 15 $°C \cdot min^{-1}$. The flame speed of the samples was measured using an IX Cameras i-SPEED 210 instrument with a pressure of 1 MPa under a nitrogen atmosphere.

3. Results and discussion

3.1. Formula optimization of Al@AP/PVDF composites

In order to obtain the potential highest energy of the MICs, the formulation of the Al@AP/PVDF composites was first determined using an optimal ratio. When the content of AP was increased, the PVDF could not hold the AP part, and large uneven particles were formed (Fig. 1(a)). As illustrated in Fig. 1(b), when the mass ratio of AP/PVDF was 1:1, the morphology of the particles looked like homogeneous particles with the maximum content of AP in the system. Therefore, the mass ratio of AP/PVDF was fixed at 1:1, since the AP could be dispersed in the PVDF polymer chains to obtain better particles with a smooth surface.

The content of the metal fuel was considered in the next step. Al@AP/PVDF mixtures with varied n-Al content (n-Al mass contents of 0, 10%, 24.5%, 33.3%, 36.2%, 50%, and 66.7%) were prepared by mechanical mixing. The heat release of the mixtures was measured by bomb calorimetry under an argon atmosphere at 3.0 MPa. (Detailed data is plotted in Fig. 2.) The experimental data was fitted by a Gaussian function to predict the best ratio of Al. The optimal content of the mass fraction of Al was found to be 33.8% (shown in Fig. 2; $R^2 = 0.98$) due to its maximum heat release. In PVDF/CuO/Al composites [27], the system has a maximum heat release value when the mass content of PVDF is 36.81%. However, when CuO is replaced by AP, the mass content of the PVDF decreases to 33.3%. The heat release and component content of the MICs differs

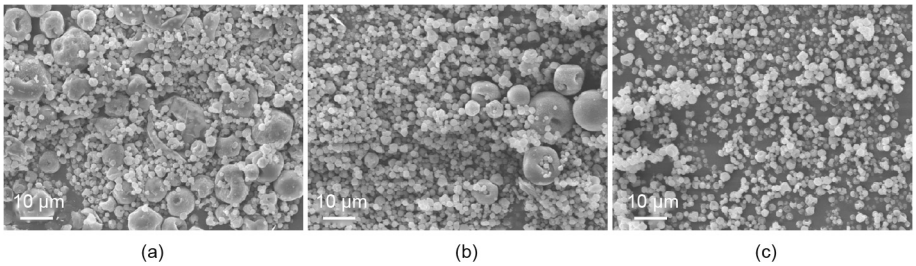

Fig. 1. Scanning electron microscopy (SEM) images of the AP/PVDF composites prepared by means of spray granulation for an AP/PVDF mass ratio of (a) 2:1, (b) 1:1, and (c) 1:2.

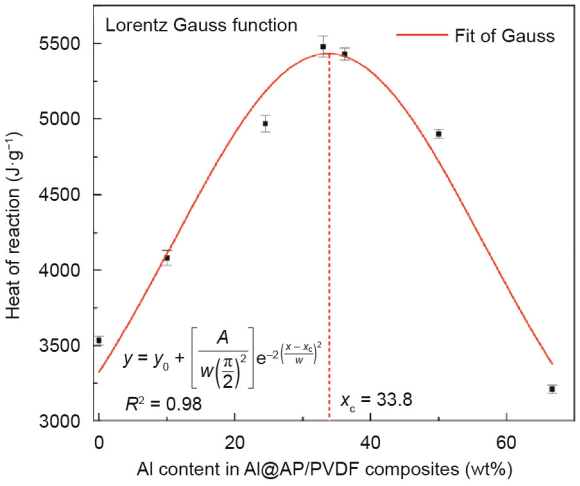

Fig. 2. Dependence of the heat of reaction on the Al mass content in Al@AP/PVDF composites. y_0: offset; A: area; w: half of the width; x_c: center of the peak.

significantly depending on the type of oxidizer. In order to obtain better division of the components, the optimal Al mass content was determined to be 33.3%, based on which the greatest efficiency and heat of reaction could be obtained. The mass ratio of Al:AP:PVDF was confirmed to be 1:1:1, and was then used to fabricate composites with the inclusion of GO as a dopant by means of the spray-drying technique.

3.2. Structure and morphology of Al@AP/PVDF and Al@AP/PVDF-GO nanocomposites

In order to enhance the energy output and combustion performance, GO was introduced and doped into Al@AP/PVDF by means of the spray granulation method. The components of these MIC mixtures are summarized in Table 1. The morphologies of the Al@AP/PVDF composites were characterized by scanning electron microscopy (SEM). Image J was used to measure the size of the composite particles, and over 200 particles were measured in each sample. As shown in Fig. 3, the Al@AP/PVDF nanoparticles are distributed evenly, and a few n-Al particles are accumulated loosely and separately. Most of the Al and GO are embedded into the AP/PVDF matrix, forming the Al@AP/PVDF-GO core–shell structure. These particles have achieved close contact between the metal fuel and the oxidizer on the nanoscale. The particle sizes are in the range of 2–4 μm. A small amount of GO doping is beneficial for the dispersion of the components and for the round morphology of the composite particles. When the GO content is increased further, however, some irregular GO flakes are distributed among the particles. These results demonstrate that GO was successfully doped into the Al@AP/PVDF composites, and that a specific ratio of GO improved the dispersion and surface structure of the Al@AP/PVDF-GO nanoparticles.

3.3. Effect of GO content on the density and reaction heat f Al@AP/PVDF nanocomposite

Density is very important for EM applications. In this research, density was tested by a gas pycnometry analyzer with a helium pressure of 0.15 MPa. Fig. 4 shows the relationship between the density and the GO content doped in Al@AP/PVDF-GO nanocomposites. It can be seen that the density increases with an increase of GO content (from 0 to 0.2%), and reaches a maximum value of 2.57 $g \cdot cm^{-3}$. However, when the GO content is increased further from 0.2% to 0.5%, the density decreases. Thus, it can be concluded that doping with GO can help to improve the density, but excessive GO addition may lead to a decrement in density. The results reveal that Al@AP/PVDF composites with 0.2% GO have the maximum density, which is 28.6% higher than that of Al@AP/PVDF without GO.

The heat of reaction of GO-doped Al@AP/PVDF was also tested, and the results are shown in Fig. 4. As shown in the figure, the heat of reaction of Al@AP/PVDF-GO is 7.3%–7.7% higher than that of Al@AP/PVDF without GO. With the addition of 0.2% GO, the energy release of Al@AP/PVDF has the maximum value of 5999.5 $J \cdot g^{-1}$. Furthermore, the heat release from the Al@AP/PVDF (5569.8 $J \cdot g^{-1}$) composite fabricated by means of spray granulation is higher than the sample made by means of mechanical mixing (5481.5 $J \cdot g^{-1}$; Fig. 2) with the same formulation. This result suggests that the improved contact between components that occurs during spray granulation improves the energy release efficiency. More importantly, the addition of GO enhances both the density and the heat release.

Table 1
Compositions of the Al@AP/PVDF-GO mixtures.

Mixture	Compositions (wt%)			
	GO	AP	Al	PVDF
Al@AP/PVDF	—	33.33	33.33	33.33
Al@AP/PVDF-$GO_{0.1}$	0.10	33.30	33.30	33.30
Al@AP/PVDF-$GO_{0.2}$	0.20	33.26	33.27	33.27
Al@AP/PVDF-$GO_{0.5}$	0.50	33.16	33.17	33.17

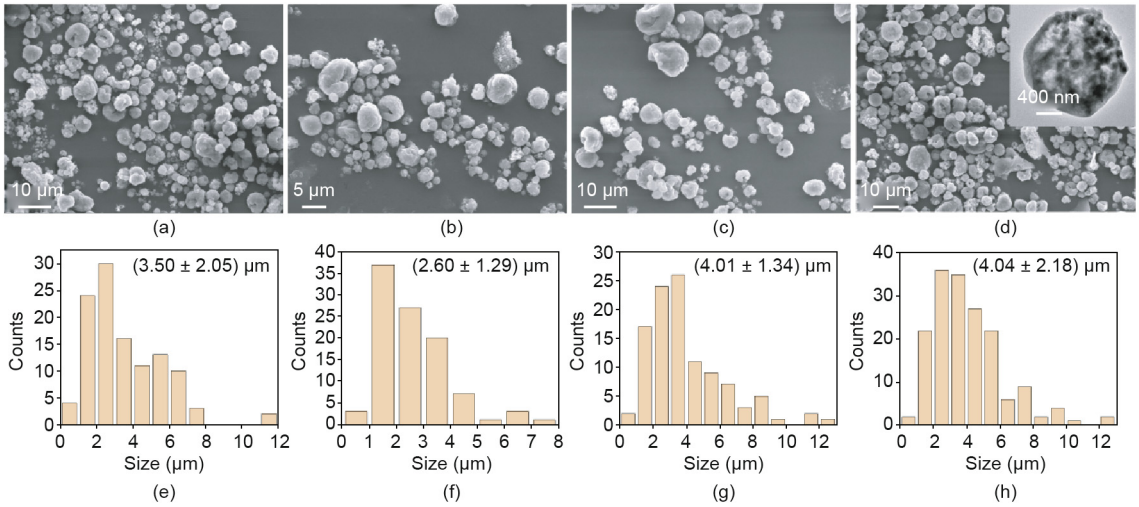

Fig. 3. Morphologies and distributions of the particles sizes of the involved materials. (a) Morphologies of the particles sizes of Al@AP/PVDF; (b) morphologies of the particles sizes of Al@AP/PVDF-$GO_{0.1}$; (c) morphologies of the particles sizes of Al@AP/PVDF-$GO_{0.2}$; (d) morphologies of the particles sizes of Al@AP/PVDF-$GO_{0.5}$; (e) distributions of the particles sizes of Al@AP/PVDF; (f) distributions of the particles sizes of Al@AP/PVDF-$GO_{0.1}$; (g) distributions of the particles sizes of Al@AP/PVDF-$GO_{0.2}$; (h) distributions of the particles sizes of Al@AP/PVDF-$GO_{0.5}$.

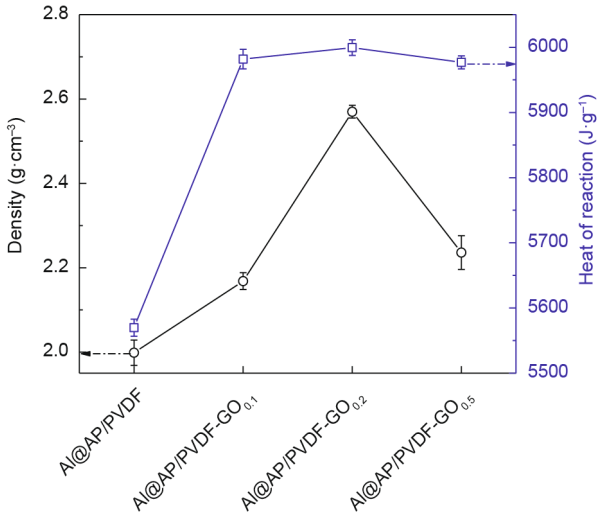

Fig. 4. Dependence of the density and reaction heat of Al@AP/PVDF on GO content.

3.4. Thermal reactivity of Al@AP/PVDF doped with GO

3.4.1. Mass loss properties of Al@AP/PVDF-GO composites

The thermogravimetry/differential thermalgravity (TG/DTG) curves of the Al@AP/PVDF-GO composites are shown in Fig. 5 and the parameters are summarized in Table 2. Only one decomposition step with around 40% mass loss at 310 °C can be observed in Fig. 5, which is due to the decomposition of AP and the reaction between fluorine and the alumina shell of the Al nanoparticles. For the mass loss process, the large slope indicates the AP decomposition. However, with the addition of GO, a small slope can be seen at a temperature range of 350–450 °C, corresponding to the reaction between fluorine and alumina.

With an increase of GO content from 0 to 0.5%, the mass loss of the composites is 39.4%, 46.4%, 42.3%, and 40.4% from 230 to 450 °C, respectively. For Al@AP/PVDF doped with GO, the uncontrollable reaction onset temperature and the peak temperature of the mass loss rate slightly shift to a lower temperature, suggesting that GO has a catalytic effect on the decomposition process of the composite particles. Moreover, the mass loss is increased with the presence of GO, indicating a better reaction efficiency. The addition of GO also has a stabilization effect on the composition decomposition by postponing the initial temperature.

3.4.2. Reaction heat effect of Al@AP/PVDF-GO composites

In order to further study the energy output of Al@AP/PVDF doped with GO, the thermal decomposition was studied by means of DSC. Fig. 6 shows the DSC curves of Al@AP/PVDF doped with GO at a heating rate of 15 °C·min^{-1}; the DSC parameters are summarized in Table 3. There are two exothermic peaks (about 315 °C and about 800 °C) and one endothermic peak (about 650 °C). Pure AP has one endothermic peak due to the phase transition at 181.3 °C and two exothermic peaks for low-temperature and high-temperature decomposition (243.0 and 286.9 °C, respectively). The decomposition of PVDF shows one endothermic peak at 165.2 °C and two exothermic peaks at 508.1 and 736.5 °C. For the decomposition of AP/PVDF, however, there are two endothermic peaks corresponding to the polymorphic transition of PVDF and AP, where the endothermic peak of PVDF decreases by about 2 °C and that of AP is postponed by around 70 °C. More interestingly, the two exothermic peaks of AP and the exothermic peak of PVDF are combined into one exothermic peak at 348.8 °C. The exothermic peak at 777.3 °C is greatly weakened with the addition of AP, compared with the peak of pure PVDF. This suggests that the interaction between AP and PVDF significantly changes the thermal decomposition mechanism of both components, so that the final composite shows the characteristics of a homogeneous PVDF/AP composite as a single compound.

In comparison, for Al@AP/PVDF and Al@AP/PVDF-GO, there is only one exothermic peak between 314 and 318 °C, depending on the content of GO. This result indicates that the presence of Al has a catalytic effect on the decomposition of the AP/PVDF composite. Moreover, GO promotes the decomposition of Al@AP/PVDF by decreasing the initial temperature. The first exothermic peak is attributed to the thermolysis of AP and the melting of the polymer, enabling the reaction of fluorine with the alumina shell of the Al. A solid–liquid transformation then occurs, and the melting peak of Al is between 645 and 666 °C. In comparison with pure Al (Fig. 6(j)), the endothermic peak of Al/PVDF decreases by 6 °C and the melting enthalpy of Al in Al/PVDF shows a large decrease, from −385.5 to −33.1 J·g^{-1}. For Al@AP/PVDF, the endothermic peak is postponed

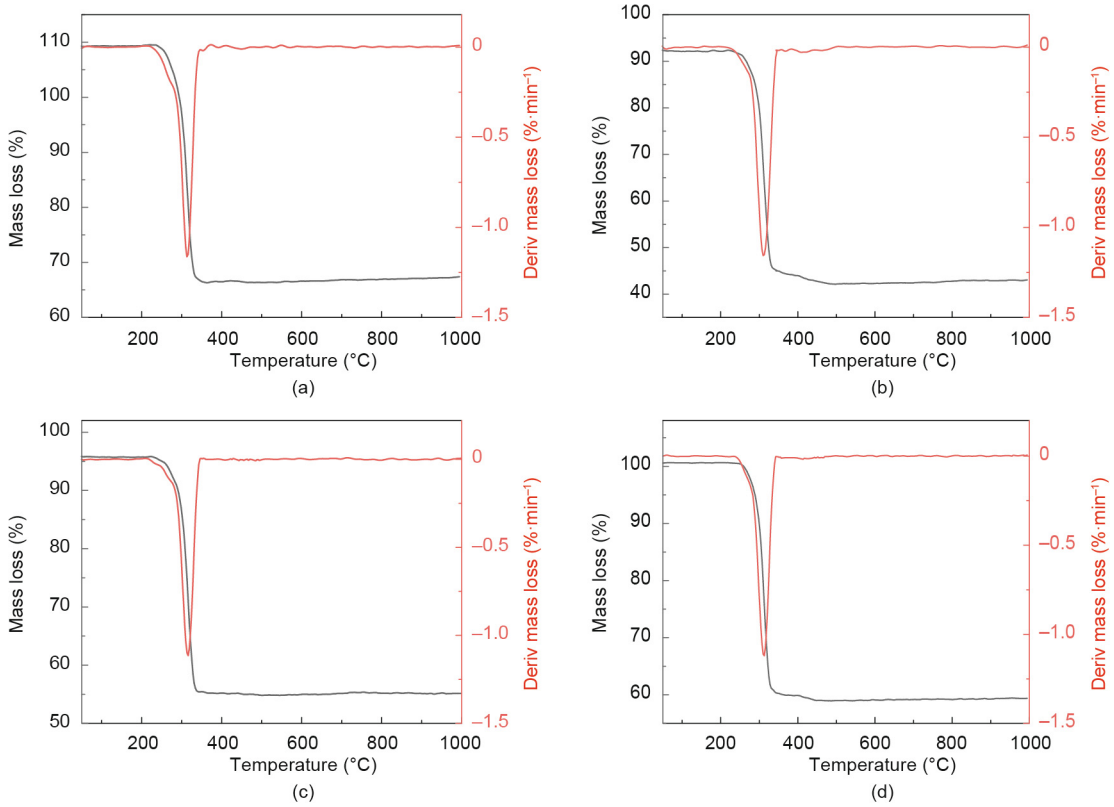

Fig. 5. TG/DTG curves of Al@AP/PVDF with/without GO at a heating rate of 15 °C·min^{-1}. (a) Al@AP/PVDF; (b) Al@AP/PVDF-$GO_{0.1}$; (c) Al@AP/PVDF-$GO_{0.2}$; (d) Al@AP/PVDF-$GO_{0.5}$.

Table 2
TG/DTG parameters of Al@AP/PVDF with GO modified at a heating rate of 15 °C·min^{-1}.

Sample	TG curves				DTG peaks	
	T_i (°C)	T_e (°C)	T_o (°C)	Mass loss (%)	T_p (°C)	L_{max} (%·min^{-1})
Al@AP/PVDF	301.1	325.4	317.0	39.4	324.9	−1.161
Al@AP/PVDF-$GO_{0.1}$	303.5	322.7	316.8	46.4	309.7	−1.154
Al@AP/PVDF-$GO_{0.2}$	301.6	329.7	312.1	42.3	316.1	−1.113
Al@AP/PVDF-$GO_{0.5}$	301.8	323.0	316.0	40.4	311.3	−1.120

T_i: initial temperature; T_e: the end temperature of mass loss; T_o: uncontrollable reaction onset temperature; T_p: peak temperature of the mass loss rate; L_{max}: maximum mass loss rate.

by around 7 °C and the melting enthalpy decreases to one third of the original.

With the addition of GO, however, the endothermic peak of Al@AP/PVDF-GO decreases by 7–14 °C and there is a very small melting enthalpy, depending on the content of GO. This result is due to the presence of the other components as impurities, which can promote the melting of Al particles under relatively low enthalpy. However, an excessive amount of GO may have a negative effect on the morphology of the composites particles, as it will result in the aggregation of Al nanoparticles outside of the composites.

The high-temperature stage is considered to be a thermite reaction with no mass loss, which corresponds to the final exothermic peak in Fig. 5. As reported by DeLisio et al. [28], the thermite reaction of Al/PVDF occurs with a peak of 770 °C, which mainly indicates the formation of hydrogen fluoride cations (HF^+), and a peak at 890 °C, which indicates the scission of the residue PVDF chains. When Al@AP/PVDF and Al@AP/PVDF-GO are compared, the exothermic decomposition of the residual PVDF and the solid-state reaction of the Al/PVDF merge into a single peak at approximately 806 °C. However, when the GO content is as high as 0.5%, the exothermic peak of the reaction between Al and PVDF decreases to a slightly lower temperature of 788.7 °C, since excessive GO may lead to aggregation problems of n-Al. This result is due to the excellent thermal conductivity and unique electronic structure of GO, which can enhance the heat-transfer process and the dispersion of the heat generated during the solid-state reactions. It is therefore logical for GO to have a stabilization effect on the decomposition of PVDF, which increases the reaction peak temperature of Al/PVDF by around 20 °C.

To further elaborate the change of the thermal decomposition mechanism, we superimposed the peaks of Figs. 6(f) and (h) over the obtained peaks shown in Fig. 6(e). Compared with the DSC curves of the involved composites made by spray granulation (Fig. 6(d)), the decomposition peaks of AP and PVDF merge into a single peak at around 318.7 °C. Two exothermic peaks, corresponding to the thermic reaction between Al and PVDF and the decomposition of PVDF, also merge into a peak at 790.8 °C. The significant differences in these two curves (Figs. 6(d) and (e)) indicate that there are completely new solid-state reaction mechanisms for the Al@AP/PVDF composite.

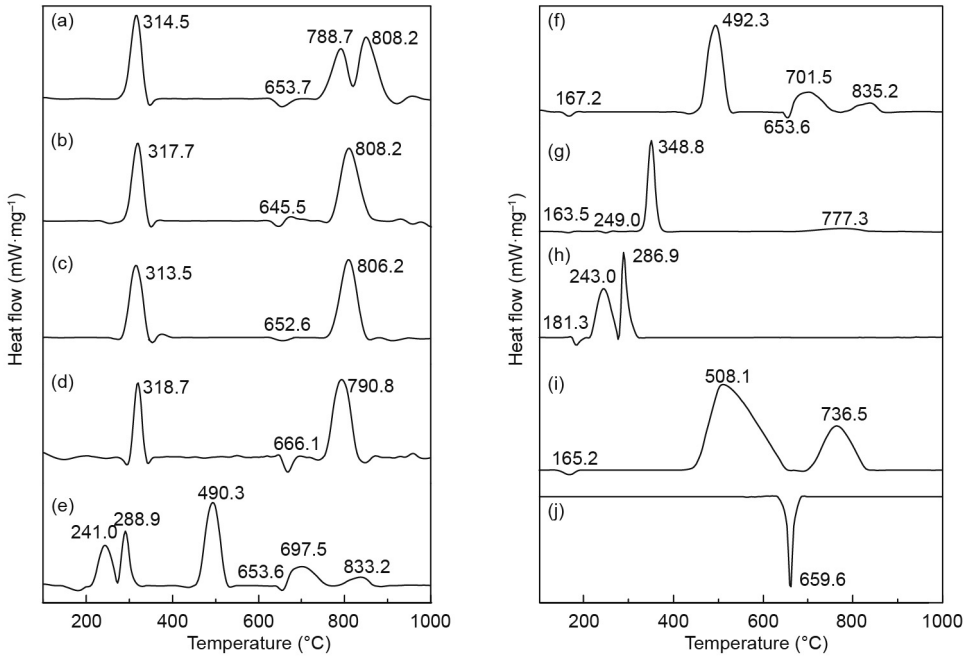

Fig. 6. Non-isothermal DSC curves of Al@AP/PVDF with varying GO concentration under a heating rate of 15 °C·min^{-1} ("by math" means that this curve was obtained by manually adding the DSC curves of Al/PVDF and pure AP at a ratio of 2:1, showing the strong interaction of these components). (a) Al@AP/PVDF-$GO_{0.5}$; (b) Al@AP/PVDF-$GO_{0.2}$; (c) Al@AP/PVDF-$GO_{0.1}$; (d) Al@AP/PVDF; (e) Al@AP/PVDF by math; (f) Al/PVDF; (g) AP/PVDF; (h) AP; (i) PVDF; (j) Al.

Table 3
DSC parameters of Al@AP/PVDF-GO composites at a heating rate of 15 °C·min^{-1}.

Sample	Endothermic peaks				Exothermic peaks				Step
	T_i (°C)	$T_{p,thermal}$ (°C)	$T_{e,heat}$ (°C)	ΔH_1 (J·g^{-1})	T_i (°C)	$T_{p,thermal}$ (°C)	$T_{e,heat}$ (°C)	ΔH_2 (J·g^{-1})	
Al@AP/PVDF	643.8	666.1	691.2	−16.6	295.2	318.7	341.3	481.9	I
					736.6	790.8	843.5	1414.0	II
Al@AP/PVDF-$GO_{0.1}$	618.0	652.6	685.2	−8.5	269.3	313.3	352.8	748.6	I
					742.6	806.2	857.3	1154.0	II
Al@AP/PVDF-$GO_{0.2}$	622.0	645.5	671.4	−7.2	266.3	317.7	350.1	610.6	I
					752.4	808.2	882.9	1113.0	II
Al@AP/PVDF-$GO_{0.5}$	627.0	653.7	693.2	−20.4	260.5	314.5	344.3	859.4	I
					736.6	788.7	814.4	437.6	II
					814.4	808.2	918.5	1068.0	III
Al/PVDF	140.7	167.2	176.2	−39.5	495.2	492.3	520.0	944.8	I
	651.5	653.6	660.2	−33.1	676.1	701.5	749.6	236.5	II
					796.9	835.2	856.1	112.5	III
AP/PVDF	142.8	163.5	171.8	−23.6	337.7	348.8	360.7	1505.0	I
	238.9	249.0	255.1	−16.8	716.7	777.3	889.4	455.4	II
Al	652.8	659.6	664.3	−385.5	—	—	—	—	I
PVDF	159.8	165.2	172.8	−18.2	459.5	508.1	592.3	4255.0	I
					707.4	736.5	820.7	1382.0	II
AP	172.2	181.3	211.4	−65.3	211.4	243.0	277.8	697.5	I
					277.8	286.9	295.5	573.3	II

$T_{p,thermal}$: peak temperature of thermal events; $T_{e,heat}$: the end temperature for heat change; ΔH_1: heat absorption; ΔH_2: heat release.

3.5. Combustion properties of Al@AP/PVDF modified with GO

The combustion characteristics of Al@AP/PVDF modified with GO were examined by testing the flame propagation speed using a high-speed camera. Fig. 7 shows sequential snapshots from a high-speed camera recording the combustion processes of the Al@AP/PVDF composites. The flame propagation speed of four samples was calculated as 4.30, 4.71, 4.76, and 4.00 m·s^{-1}, respectively. The flame speed of the composites doped with GO was increased by 10.7% in comparison with that of Al@AP/PVDF. However, when the GO content reached 0.5%, the burning rate decreased and the excessive GO caused uneven distribution in the composite system, resulting in a lower burn rate. The positive effect of GO on combustion speed may be attributed to its rapid heat-transfer process, which has a strong catalytic effect on the decomposition of AP and PVDF.

The Al@AP/PVDF-GO composite (5 mg) was placed in an alumina pot under a nitrogen atmosphere. A CO_2 laser igniter (4 V of ignition voltage and 12 s of heating time), a spectrometer (Avasoec-2048, Avantes, the Netherlands), and a high-speed camera were installed in order to simultaneously record the optical history and combustion process. In general, the features seen in the spectra in Fig. 8 are representative of what was seen for all experiments. The peaks near 590 and 767 nm correspond to the emission of AlO (g) and NH_4Cl (g), respectively. The addition of GO may increase the peak intensity of AlO and NH_4Cl. However,

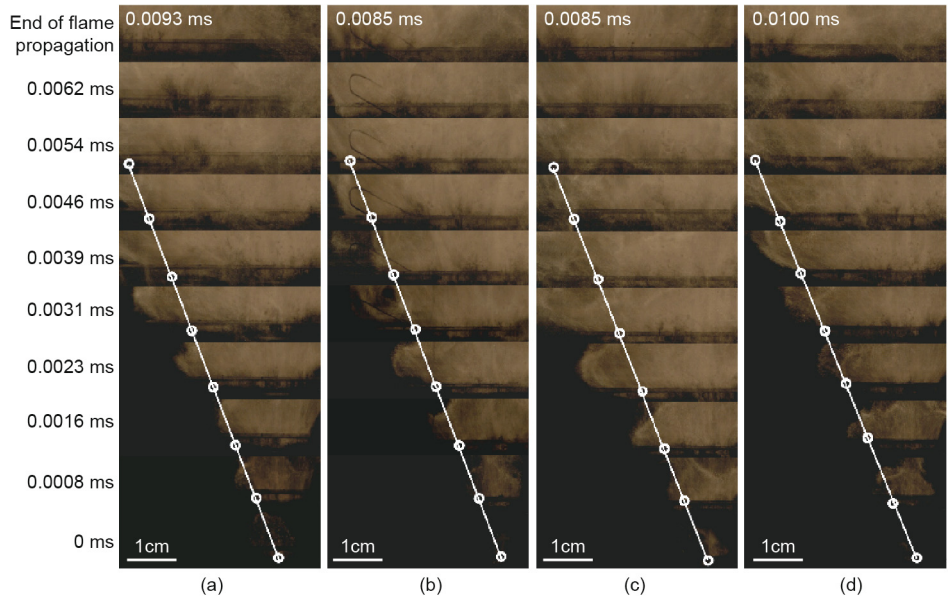

Fig. 7. Screenshot flame propagation images from a high speed camera. (a) Al@AP/PVDF; (b) Al@AP/PVDF-$GO_{0.1}$; (c) Al@AP/PVDF-$GO_{0.2}$; (d) Al@AP/PVDF-$GO_{0.5}$.

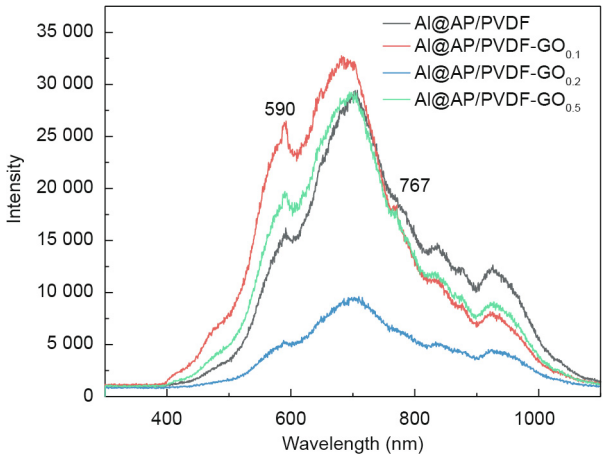

Fig. 8. Typical emission spectra of Al@AP/PVDF-GO composites in discernible time.

the emission of AlO (g) is at the minimum for the sample with 0.2% of GO doping, in which the reaction between Al and H–F dominates the oxidation process.

Fig. 9 shows the condensed combustion products of Al@AP/PVDF-GO, and exhibits the aggregation of the disordered particles. It can be seen from Fig. 9(a) that the morphology of the products of Al@AP/PVDF-GO shows severe agglomerations. With an appropriate addition of GO, the agglomeration performance can be improved, as shown in Figs. 9(b) and (c). Moreover, a large amount of GO nanosheets can be observed in Fig. 9(d), due to the over-doping of GO. Composite particles doped with GO show increased reactivities and are more sensitive to thermal decomposition; the agglomeration size is also decreased. These results further demonstrate that GO doping improves the combustion rate and efficiency.

The condensed combustion products were determined by means of powder XRD in order to identify the possible combustion reaction mechanisms. These nano-metal particles are mainly AlF_3, AlN, Al_2O_3, and Al, as detected by XRD (Fig. 10), indicating that most of the n-Al is consumed during the reaction process. Al reacts with AP or PVDF to generate the products AlF_3 and AlN. It is postulated that the decomposition reactions of the Al@AP/PVDF composite are as follows:

$$2(-CH_2-CF_2)_n \rightarrow 2HF + CH_2 + CF_2 + 2C$$

$$Al_2O_3 + 6HF \rightarrow 2AlF_3 + 3H_2O$$

$$2Al + 3(-CH_2-CF_2)_n \rightarrow 3H_2 + 2AlF_3 + 6C$$

$$2NH_4ClO_4 \rightarrow N_2 + 4H_2O + Cl_2 + 2O_2$$

$$6Al + N_2 + 3O_2 \rightarrow 2AlN + 2Al_2O_3$$

In addition, the peak intensity of Al and Al_2O_3 became weaker with the addition of GO in comparison with Al@AP/PVDF, which is consistent with the reduction in the AlO emission intensity shown in Fig. 8. This finding suggests that better combustion efficiency can be achieved by GO modification.

4. Conclusions

In summary, Al@AP/PVDF nanoparticles were successfully prepared by means of spray granulation, and the optimized formulation of Al@AP/PVDF was determined to be a mass ratio of 1:1:1, which had the highest energy output (5478.1 $J \cdot g^{-1}$). The effect of GO content (0.1%, 0.2%, and 0.5%) was also investigated, and the following conclusions were made:

(1) It was found that Al@AP/PVDF-$GO_{0.2}$ has the highest density (2.57 $g \cdot cm^{-3}$) and highest heat of reaction (5999.5 $J \cdot g^{-1}$) in comparison with the other Al@AP/PVDF nanoparticles. This Al@AP/PVDF compound has only one exothermic peak around 318 °C, which is attributed to the thermolysis of AP and the melting of the polymer enabling the reaction of fluorine with the alumina shell of the Al. Al melting then occurs at about 650 °C. The addition of GO decreases the temperature of these two peaks, depending on the content of GO. After that, one exothermic decomposition peak occurs at approximately 806 °C, which corresponds to the thermite reaction between Al and PVDF and the decomposition reaction of the residual PVDF. The presence of GO has a stabilization effect on this exothermic peak. However, when the GO content increases

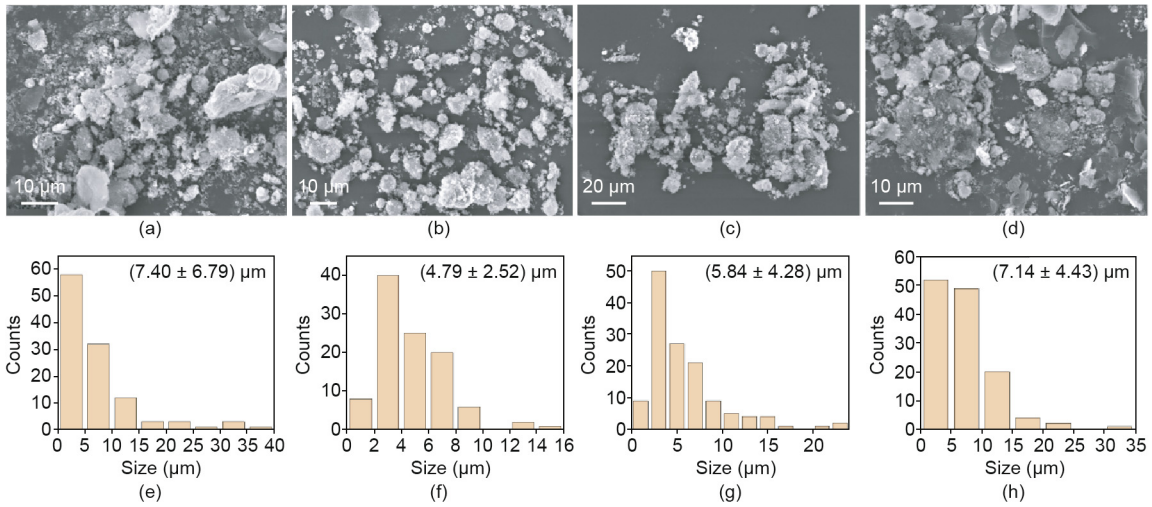

Fig. 9. SEM images and distributions of the particle sizes of the condensed combustion products. (a) SEM images of the particle sizes of Al@AP/PVDF; (b) SEM images of the particle sizes of Al@AP/PVDF-$GO_{0.1}$; (c) SEM images of the particle sizes of Al@AP/PVDF-$GO_{0.2}$; (d) SEM images of the particle sizes of Al@AP/PVDF-$GO_{0.5}$; (e) distributions of the particle sizes of Al@AP/PVDF; (f) distributions of the particle sizes of Al@AP/PVDF-$GO_{0.1}$; (g) distributions of the particle sizes of Al@AP/PVDF-$GO_{0.2}$; (h) distributions of the particle sizes of Al@AP/PVDF-$GO_{0.5}$.

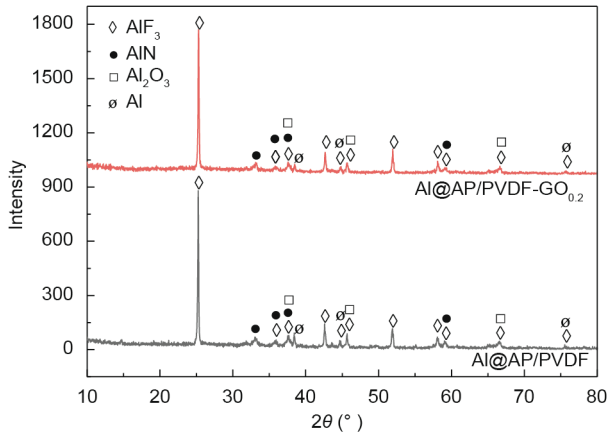

Fig. 10. XRD spectra of the combustion residues after the calorimetry bomb of Al@AP/PVDF with or without GO. 2θ: diffraction angle.

to 0.5%, the exothermic peak of the reaction between Al and PVDF decreases to a slightly lower temperature of 788.7 °C due to the aggregation problem. Moreover, two exothermic peaks of AP and one exothermic peak of PVDF are combined into a single exothermic peak at around 318 °C due to the interaction between AP and PVDF, indicating the characteristics of the homogeneous AP/PVDF composite as a single compound.

(2) GO has a catalytic effect on the thermite reaction of the Al@AP/PVDF composite, and a stabilization effect on the decomposition of AP and PVDF.

(3) Doping 0.2% GO can greatly improve the energy output and enhance the combustion speed of Al@AP/PVDF, due to the improved contact and distribution of the components for the composite structure of Al@AP/PVDF-GO. The highest flame speed (4.76 $m \cdot s^{-1}$) was obtained when the content of GO was 0.2%. Doping an excessive amount of GO would lead to a decrease in reaction efficiency, and therefore to a lower burn rate.

Acknowledgements

This work was supported by the National Natural Science Foundation of China (51776176) and the Fundamental Research Funds for the Central Universities, China (G2017KY0301).

Compliance with ethics guidelines

Shuwen Chen, De-Yun Tang, Xue-Xue Zhang, Jie-Yao Lyu, Wei He, Peijin Liu, and Qi-Long Yan declare that they have no conflict of interest or financial conflicts to disclose.

References

[1] He W, Liu PJ, He GQ, Gozin M, Yan QL. Highly reactive metastable intermixed composites (MICs): preparation and characterization. Adv Mater 2018;30(41):1706293.
[2] Bockmon BS, Pantoya ML, Son SF, Asay BW, Mang JT. Combustion velocities and propagation mechanisms of metastable interstitial composites. J Appl Phys 2005;98(6):064903.
[3] Yan QL, Zhao FQ, Kuo KK, Zhang XH, Zeman S, DeLuca LT. Catalytic effects of nano additives on decomposition and combustion of RDX- HMX-, and AP-based energetic compositions. Prog Energ Combust Sci 2016;57:75–136.
[4] Yan QL, Gozin M, Zhao FQ, Cohen A, Pang SP. Highly energetic compositions based on functionalized carbon nanomaterials. Nanoscale 2016;8(9):4799–851.
[5] Asay BW, Son SF, Busse JR, Oschwald DM. Ignition characteristics of metastable intermolecular composites. Propellants Explos Pyrotech 2010;29(4):216–9.
[6] Siegert B, Comet M, Muller O, Pourroy G, Spitze D. Reduced-sensitivity nanothermites containing manganese oxide filled carbon nanofibers. J Phys Chem C 2010;114(46):19562–8.
[7] Yu C, Zhang W, Shen R, Xu X, Cheng J, Ye JH, et al. Tunable microwave absorption in Co–Al substituted M-type Ba–Sr hexagonal ferrite. Mater Des 2016;110:749–61.
[8] Gao K, Li G, Luo Y, Wang L, Shen L, Wang G. Preparation and characterization of the AP/Al/Fe_2O_3 ternary nano-thermites. J Therm Anal Calorim 2014;118(1):43–9.
[9] Joshi A, Mer KKS, Bhattacharya S, Patel VK. Nano-aluminium as catalyst in thermal decomposition of energetic materials. In: Bhattacharya S, Agarwal A, Rajagopalan T, Patel V, editors. Nano-energetic materials. Singapore: Springer; 2019. p. 109–20.
[10] Zhu YL, Huang H, Ren H, Jiao QL. Influence of aluminum particle size on thermal decomposition of RDX. J Energ Mater 2013;31(3):178–91.
[11] Sadeghipour S, Ghaderian J, Wahid MA. Advances in aluminum powder usage as an energetic material and applications for rocket propellant. In: Proceedings of the 4th International Meeting of Advances in Thermofluids; 2011 Oct 3–4; Melaka, Malaysia; 2012..
[12] He W, Liu P, Gong F, Tao B, Gu J, Yang Z, et al. Tuning the reactivity of metastable intermixed composite n-Al/PTFE by polydopamine interfacial control. Appl Mater Interfaces 2018;10:32849–58.
[13] He W, Ao W, Yang GC, Yang ZJ, Guo ZQ, Liu PJ, et al. Metastable energetic nanocomposites of MOF-activated aluminum featured with multi-level energy releases. Chem Eng J 2019;381:122623.
[14] Tang DY, Chen SW, Liu XL, He W, Yang GC, Liu PJ, et al. Controlled reactivity of metastable n-Al@$Bi(IO_3)_3$ by employment of tea polyphenols as an interfacial layer. Chem Eng J 2019;381:122747.
[15] Eslami A, Hosseini SG, Bazrgary M. Improvement of thermal decomposition properties of ammonium perchlorate particles using some polymer coating agents. J Therm Anal Calorim 2013;113(2):721–30.

[16] Fang C, Li S. Experimental research of the effects of superfine aluminum powders on the combustion characteristics of NEPE propellants. Propellants Explos Pyrotech 2002;27(1):34–8.
[17] Li D, Zhao F, Li S, Xu H, Li Y. Combustion property of NEPE propellant with CL-20. Chin J Energ Mater 2007;15(4):324–8.
[18] Yang V, Brill TB, Ren WZ. Solid propellant chemistry, combustion, and motor interior ballistics. Reston: American Institute of Aeronautics and Astronautics, Inc; 2000.
[19] Armstrong RW, Baschung B, Booth DW, Samirant M. Enhanced propellant combustion with nanoparticles. Nano Lett 2003;3(2):253–5.
[20] Nandagopal S, Mehilal M, Tapaswi MA, Jawalkar SN, Radhakrishnan KK, Bhattacharya B. Effect of coating of ammonium perchlorate with fluorocarbon on ballistic and sensitivity properties of AP/Al/HTPB propellant. Propellants Explos Pyrotech 2009;34(6):526–31.
[21] John HJ, Hudson FE, Robbs R. High strain rate testing of AP/Al/HTPB solid propellants. Aip Conference Process 1998;429(1):603–6.
[22] Wang H, Jacob RJ, DeLisio JB, Zachariah MR. Assembly and encapsulation of aluminum NP's within AP/NC matrix and their reactive properties. Combust Flame 2017;180:175–83.
[23] Li JZ, Fan XZ, Zhong L, Liu X. Mechanical properties of NC/NG/AP/Al composite modified double-base propellant. Chin J Energ Mater 2007;15(4):345–8.
[24] Huang S, Pan M, Deng S, Jiang Y, Zhao J, Wendt BL, et al. Modified micro-emulsion synthesis of highly dispersed Al/PVDF composites with enhanced combustion properties. Adv Eng Mater 2019;21(5):1801330.
[25] Sippel TR, Son SF, Groven LJ. Altering reactivity of aluminum with selective inclusion of polytetrafluoroethylene through mechanical activation. Propellants Explos Pyrotech 2013;38(2):286–95.
[26] Wang J, Zeng C, Zhan C, Zhang L. Tuning the reactivity and combustion characteristics of PTFE/Al through carbon nanotubes and grapheme. Thermochim Acta 2019;676:276–81.
[27] Lyu JY, Chen S, He W, Zhang XX, Tang DE, Liu PJ, et al. Fabrication of high-performance graphene oxide doped PVDF/CuO/Al nanocomposites via electrospinning. Chem Eng J 2019;368:129–37.
[28] DeLisio JB, Huang C, Jian G, Zachariah M, Young G. Ignition and reaction analysis of high loading nano-Al/fluoropolymer energetic composite films. In: Proceedings of the 52nd Aerospace Sciences Meeting; 2014 Jan 13–17; National Harbor, Washington, DC, USA; 2014.